

Synthesis, Structure, and Reactivity of Functionalized Germyl Complexes of the Formula $(\eta^5\text{-C}_5\text{H}_5)\text{Re}(\text{NO})(\text{PPh}_3)(\text{GePh}_2\text{X})$: Equilibria Involving the Germylene Complex $[(\eta^5\text{-C}_5\text{H}_5)\text{Re}(\text{NO})(\text{PPh}_3)(=\text{GePh}_2)]^+\text{TfO}^-$

Kenneth E. Lee, Atta M. Arif, and J. A. Gladysz*

Department of Chemistry, University of Utah, Salt Lake City, Utah 84112

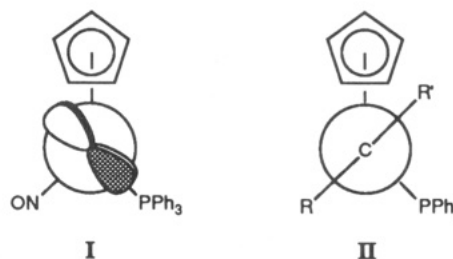
Received June 29, 1990

Reactions of $\text{Li}^+[(\eta^5\text{-C}_5\text{H}_5)\text{Re}(\text{NO})(\text{PPh}_3)]^-$ with Ph_3GeCl and Ph_2GeCl_2 (THF, -78°C) give germyl complexes $(\eta^5\text{-C}_5\text{H}_5)\text{Re}(\text{NO})(\text{PPh}_3)(\text{GePh}_3)$ (3, 84%) and $(\eta^5\text{-C}_5\text{H}_5)\text{Re}(\text{NO})(\text{PPh}_3)(\text{GePh}_2\text{Cl})$ (4, 82%). Reactions of 4 with LiAlH_4 and Me_3SiOTf give $(\eta^5\text{-C}_5\text{H}_5)\text{Re}(\text{NO})(\text{PPh}_3)(\text{GePh}_2\text{H})$ (5, 88%) and $(\eta^5\text{-C}_5\text{H}_5)\text{Re}(\text{NO})(\text{PPh}_3)(\text{GePh}_2\text{OTf})$ (6, 82%). The triflate substituent in 6 is very labile, as evidenced by rapid reactions with halide ion sources to give $(\eta^5\text{-C}_5\text{H}_5)\text{Re}(\text{NO})(\text{PPh}_3)(\text{GePh}_2\text{X})$ (X = F, Br, I; 92-94%) and with pyridine and 4-methylpyridine to give $[(\eta^5\text{-C}_5\text{H}_5)\text{Re}(\text{NO})(\text{PPh}_3)(\text{GePh}_2(4\text{-NC}_5\text{H}_4\text{R}))]^+\text{TfO}^-$ (83-76%). The ^{13}C NMR resonances of the diastereotopic germanium phenyl groups in 6 coalesce at low temperatures ($\Delta G^\ddagger(268\text{ K}, \text{CD}_2\text{Cl}_2) = 12.6\text{ kcal mol}^{-1}$). The most likely mechanisms for this dynamic behavior entail initial triflate dissociation to give the germylene complex $[(\eta^5\text{-C}_5\text{H}_5)\text{Re}(\text{NO})(\text{PPh}_3)(=\text{GePh}_2)]^+\text{TfO}^-$ (12). The crystal structure of 6 (monoclinic, $P2_1/n$ (No. 14); $a = 16.908$ (3) Å, $b = 20.160$ (3) Å, $c = 10.437$ (2) Å, $\beta = 93.82$ (2)°, $Z = 4$) exhibits features suggestive of a substantial resonance contribution by 12. Addition of $\text{HBF}_4\cdot\text{OEt}_2$ to 3 gives the hydride complex $[(\eta^5\text{-C}_5\text{H}_5)\text{Re}(\text{NO})(\text{PPh}_3)(\text{GePh}_3)(\text{H})]^+\text{BF}_4^-$ (43%), and reaction of 5 with $n\text{-BuLi}$ and then $\text{HBF}_4\cdot\text{OEt}_2$ gives the germylcyclopentadienyl complex $(\eta^5\text{-C}_5\text{H}_4\text{GePh}_2\text{H})\text{Re}(\text{NO})(\text{PPh}_3)(\text{H})$ (46%).

Transition-metal silylene and germylene complexes, $[\text{L}_n\text{M}=\text{ER}_2]^{n+}$ (E = Si, Ge; $n = 0, 1$), have been the focus of considerable recent attention.¹⁻⁴ In particular, the synthesis and isolation of stable compounds have posed a formidable challenge. In contrast, isolable metal carbene complexes, $[\text{L}_n\text{M}=\text{CR}_2]^{n+}$, are ubiquitous.

Certain metal fragments characteristically form carbene complexes that exhibit superior kinetic stability. One example is the rhenium moiety $[(\eta^5\text{-C}_5\text{H}_5)\text{Re}(\text{NO})(\text{PPh}_3)]^+$.⁵ This assembly possesses the high-lying d orbital

HOMO shown in I⁶ and is a potent π donor. The corre-



(1) Petz, W. *Chem. Rev.* 1986, 86, 1019.

(2) Base-free silylene complexes are presently unknown. Leading references to base-stabilized silylene complexes: (a) Straus, D. A.; Zhang, C.; Quimbata, G. E.; Grumbine, S. D.; Heyn, R. H.; Tilley, T. D.; Rheingold, A. L.; Geib, S. J. *J. Am. Chem. Soc.* 1990, 112, 2673. (b) Tobita, H.; Ueno, K.; Shimoi, M.; Ogino, H. *Ibid.* 1990, 112, 3415. (c) Zybilla, C.; Wilkinson, D. L.; Leis, C.; Müller, G. *Angew. Chem., Int. Ed. Engl.* 1989, 28, 203. (d) Note added in proof: A sulfur-substituted ruthenium silylene complex has been isolated: Straus, D. A.; Grumbine, S. D.; Tilley, T. D. *J. Am. Chem. Soc.* 1990, 112, 7801.

(3) Leading references to base-free germylene complexes: (a) Jutzi, P.; Steiner, W. *Angew. Chem., Int. Ed. Engl.* 1976, 15, 684; 1977, 16, 639. (b) Lappert, M. F.; Miles, S. J.; Power, P. P.; Carty, A. J.; Taylor, N. J. *J. Chem. Soc., Chem. Commun.* 1977, 458. (c) Jutzi, P.; Steiner, W.; König, E.; Huttner, G.; Frank, A.; Schubert, U. *Chem. Ber.* 1978, 111, 606. (d) Lappert, M. F.; Power, P. P. *J. Chem. Soc., Dalton Trans.* 1985, 51. (e) Jutzi, P.; Hampel, B.; Stroppel, K.; Krüger, C.; Angermund, K.; Hofmann, P. *Chem. Ber.* 1985, 118, 2789. (f) Hitchcock, P. B.; Lappert, M. F.; Misra, M. C. *J. Chem. Soc., Chem. Commun.* 1985, 863. (g) Jutzi, P.; Hampel, B.; Hursthouse, M. B.; Howes, A. J. *J. Organomet. Chem.* 1986, 299, 19. (h) Hawkins, S. M.; Hitchcock, P. B.; Lappert, M. F.; Rai, A. K. *J. Chem. Soc., Chem. Commun.* 1986, 1689. (i) du Mont, W.-W.; Lange, L.; Pohl, S.; Saak, W. *Organometallics* 1990, 9, 1395.

(4) Other recent studies relevant to germylene complexes: (a) Castel, A.; Rivière, P.; Satgé, J.; Ahbala, M. *J. Organomet. Chem.* 1987, 331, 11. (b) Herrmann, W. A.; Kneuper, H.-J.; Herdtweck, E. *Chem. Ber.* 1989, 122, 433. (c) Lei, D.; Hampden-Smith, M. J. *J. Chem. Soc., Chem. Commun.* 1989, 1211. (d) Borvornwattananont, A.; Moller, K.; Bein, T. *Ibid.* 1990, 28. (e) Barsuaskas, G.; Lei, D.; Hampden-Smith, M. J.; Duesler, E. N. *Polyhedron* 1990, 9, 773. (f) Review of multiply bonded germanium species: Barrau, J.; Escudié, J.; Satgé, J. *Chem. Rev.* 1990, 90, 283.

(5) (a) Kiel, W. A.; Lin, G.-Y.; Constable, A. G.; McCormick, F. B.; Strouse, C. E.; Eisenstein, O.; Gladysz, J. A. *J. Am. Chem. Soc.* 1982, 104, 4865. (b) Kiel, W. A.; Lin, G.-Y.; Bodner, G. S.; Gladysz, J. A. *Ibid.* 1983, 105, 4958. (c) Patton, A. T.; Strouse, C. E.; Knobler, C. B.; Gladysz, J. A. *Ibid.* 1983, 105, 5804. (d) Merrifield, J. H.; Lin, G.-Y.; Kiel, W. A.; Gladysz, J. A. *Ibid.* 1983, 105, 5811. (e) Kiel, W. A.; Buhro, W. E.; Gladysz, J. A. *Organometallics* 1984, 3, 879. (f) O'Connor, E. J.; Kobayashi, M.; Floss, H. G.; Gladysz, J. A. *J. Am. Chem. Soc.* 1987, 109, 4837.

sponding alkylidene complexes $[(\eta^5\text{-C}_5\text{H}_5)\text{Re}(\text{NO})(\text{PPh}_3)(=\text{CRR}')^+\text{X}^-$ have proved easily isolable. Crystal structures show the $\text{Re}=\text{C}$ conformation depicted in idealized projection II.^{5a,c} This ligand orientation maximizes overlap of the d orbital shown in I with the vacant p acceptor orbital on C_α . NMR experiments give $\text{Re}=\text{C}$ rotational barriers of 18-21 kcal/mol.⁵

We therefore sought to probe the accessibility of analogous cationic germylene complexes, $[(\eta^5\text{-C}_5\text{H}_5)\text{Re}(\text{NO})(\text{PPh}_3)(=\text{GeR}_2)]^+\text{X}^-$. In this paper, we report (1) the high-yield synthesis of a series of functionalized diphenylgermyl complexes, $(\eta^5\text{-C}_5\text{H}_5)\text{Re}(\text{NO})(\text{PPh}_3)(\text{GePh}_2\text{X})$, (2) structural, dynamic NMR, and chemical properties that provide good evidence for equilibria with germylene complexes, and (3) other exploratory reactions directed toward germylene complex targets. A portion of this work has been communicated.⁷

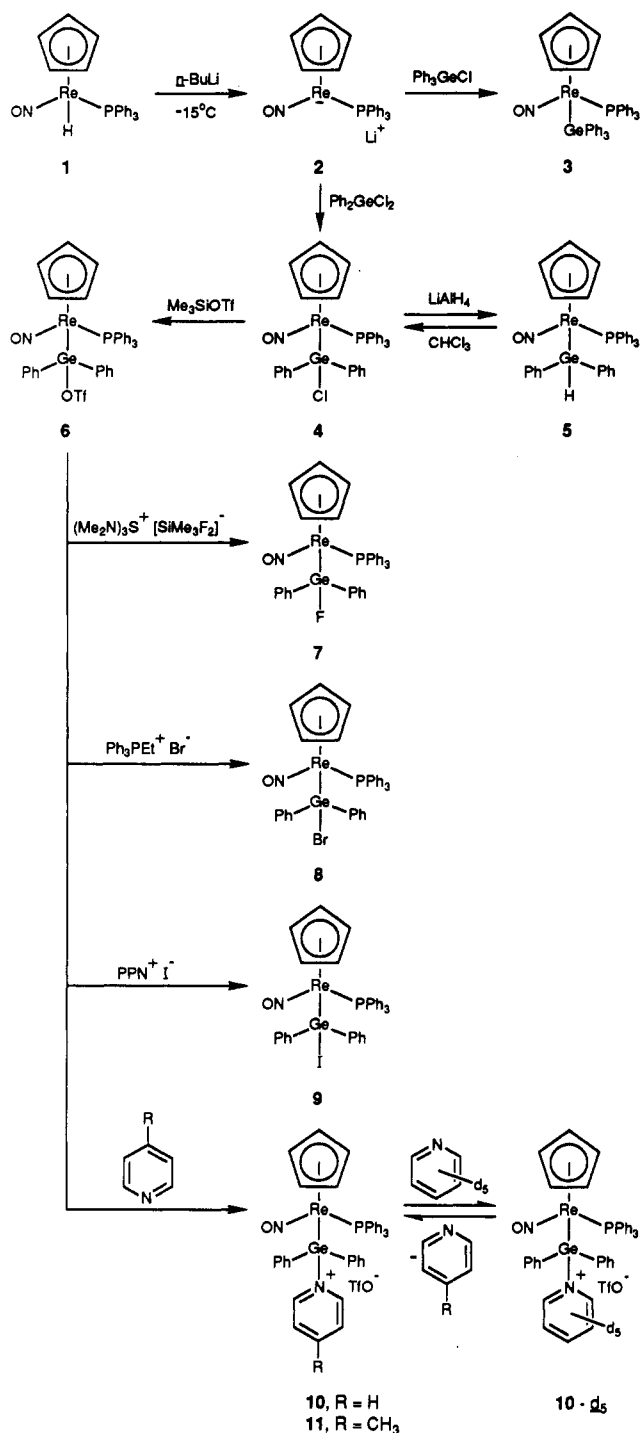
Results

1. Synthesis of Diphenylgermyl Complexes. The hydride complex $(\eta^5\text{-C}_5\text{H}_5)\text{Re}(\text{NO})(\text{PPh}_3)(\text{H})$ (1) and $n\text{-BuLi}$ (1.1 equiv) were reacted in THF at -15°C as previously described to give the "anion" $\text{Li}^+[(\eta^5\text{-C}_5\text{H}_5)\text{Re}(\text{NO})(\text{PPh}_3)]^-$ (2).⁸ The electrophiles Ph_3GeCl and

(6) (a) Schilling, B. E. R.; Hoffmann, R.; Faller, J. *J. Am. Chem. Soc.* 1979, 101, 592. (b) Georgiou, S.; Gladysz, J. A. *Tetrahedron* 1986, 42, 1109.

(7) Lee, K. E.; Gladysz, J. A. *Polyhedron* 1988, 7, 2209.

Scheme I. Syntheses of the Functionalized Diphenylgermyl Complexes
 $(\eta^5\text{-C}_5\text{H}_5)\text{Re}(\text{NO})(\text{PPh}_3)(\text{GePh}_2\text{X})$



Ph_2GeCl_2 were subsequently added. Workup gave the corresponding germyl complexes $(\eta^5\text{-C}_5\text{H}_5)\text{Re}(\text{NO})(\text{PPh}_3)(\text{GePh}_3)$ (3) and $(\eta^5\text{-C}_5\text{H}_5)\text{Re}(\text{NO})(\text{PPh}_3)(\text{GePh}_2\text{Cl})$ (4) in 84% and 82% yields, respectively (Scheme I).

Complexes 3 and 4, and all other new compounds isolated below, were characterized by IR and NMR (^1H , $^{13}\text{C}\{^1\text{H}\}$, $^{31}\text{P}\{^1\text{H}\}$) spectroscopy (Table I). Microanalyses (Experimental Section) sometimes bordered on limits commonly associated with analytical purity—a finding ascribed to the lability of certain functionalized germyl

complexes below and/or the presence of interfering element combinations.

Both 3 and 4 exhibited distinct ^{13}C NMR resonances for the ipso, ortho, meta, and para germanium-phenyl carbons, with the ipso resonances considerably downfield from the others. Also, note that in diphenylgermyl complex 4, the germanium-phenyl groups are diastereotopic. Thus, up to eight GePh ^{13}C NMR resonances are possible. The two ipso carbons gave separate resonances (150.0, 147.8 ppm), but the other pairs of carbons were degenerate.

Other functionalized diphenylgermyl complexes were sought. Reaction of 4 and LiAlH_4 (THF, 25 °C) gave the hydridogermyl complex $(\eta^5\text{-C}_5\text{H}_5)\text{Re}(\text{NO})(\text{PPh}_3)(\text{GePh}_2\text{H})$ (5, Scheme I) in 88% yield after workup. Complex 5 exhibited a diagnostic IR ν_{GeH} absorption (1979 cm^{-1})^{9a} and a phosphorus-coupled germanium hydride ^1H NMR resonance (δ 4.97 d), as well as distinct ^{13}C NMR resonances for all carbons of the diastereotopic germanium-phenyl groups (Table I). Complex 5 was stable for extended periods in dichloromethane but reacted in chloroform over the course of 48 h to give chlorogermyl complex 4 and dichloromethane. Closely related hydridosilyl complexes undergo analogous chlorinations in chloroform.¹⁰

We sought to replace the chloride in 4 with a better leaving group. Accordingly, reaction of 4 and Me_3SiOTf (CH_2Cl_2 , 25 °C) gave the triflate-substituted germyl complex $(\eta^5\text{-C}_5\text{H}_5)\text{Re}(\text{NO})(\text{PPh}_3)(\text{GePh}_2\text{OTf})$ (6, Scheme I) in 82% yield after workup. Interestingly, identical ^{13}C NMR resonances were observed for carbons of the diastereotopic germanium-phenyl groups in ambient-temperature spectra. The ipso and ortho resonances were broadened, and variable-temperature ^{13}C NMR spectra are described below. Complex 6 exhibited a single IR ν_{NO} absorption in both KBr and CH_2Cl_2 (1678, 1683 cm^{-1}), as would be expected of a homogeneous material.

Substitution of the triflate group in 6 was attempted (Scheme I). Dichloromethane solutions of 6 were treated with the halide ion sources $(\text{Me}_2\text{N})_3\text{S}^+[\text{SiMe}_3\text{F}_2]^-$ (TASF),¹¹ $\text{Ph}_3\text{PEt}^+\text{Br}^-$, and $[\text{Ph}_3\text{P}^+\text{N}^-\text{PPh}_3]^+\text{I}^-$ (PPN⁺I⁻). Reactions were complete after 5 min at -78 °C, as assayed by ^{31}P NMR spectroscopy. Workup gave the corresponding halogermyl complexes $(\eta^5\text{-C}_5\text{H}_5)\text{Re}(\text{NO})(\text{PPh}_3)(\text{GePh}_2\text{X})$ (X = F, 7, 92%; X = Br, 8, 93%; X = I, 9, 94%). The spectroscopic data in Table I show several conspicuous trends for halogermyl complexes 7/4/8/9 (e.g., progressively downfield shifts of the cyclopentadienyl ^1H and ^{13}C NMR resonances). Note that 7-9 exhibit separate ^{13}C NMR resonances for most of the diastereotopic germanium-phenyl carbons.

Complex 6 was similarly treated with pyridine and 4-methylpyridine (Scheme I). Reactions were complete within 5 min at -78 °C, as assayed by ^{31}P NMR spectroscopy. Workup gave the adducts $[(\eta^5\text{-C}_5\text{H}_5)\text{Re}(\text{NO})(\text{PPh}_3)(\text{GePh}_2(\text{NC}_5\text{H}_4\text{R}))]^+\text{TfO}^-$ (R = H, 10, 83%; R = 4-Me, 11, 76%). The IR spectra of 10 and 11 showed a symmetric inplane pyridine C-H bending vibration at 1610-1626 cm^{-1} . This mode characteristically increases from that of free pyridine (1578 cm^{-1} , neat) in pyridinium salts and coordination compounds.¹²

Complex 10 (0.02 M in CD_2Cl_2) was treated with 2.5

(9) (a) Lesbre, M.; Mazerolles, P.; Satgé, J. *The Organic Chemistry of Germanium*; Wiley: New York, 1971; p 341. (b) *Ibid.*, p 20. (c) *Ibid.*, pp 260-261.

(10) (a) Lee, K. E.; Arif, A. M.; Gladysz, J. A. *Inorg. Chem.* 1990, 29, 2885. (b) Lee, K. E.; Arif, A. M.; Gladysz, J. A. *Chem. Ber.* 1991, 124, 309.

(11) Middleton, W. J. *Org. Synth.* 1985, 64, 221.

(12) (a) Gill, N. S.; Nuttall, R. H.; Scaife, D. E.; Sharp, D. W. A. *J. Inorg. Nucl. Chem.* 1961, 104, 141. (b) Thornton, D. A. *Coord. Chem. Rev.* 1990, 104, 251.

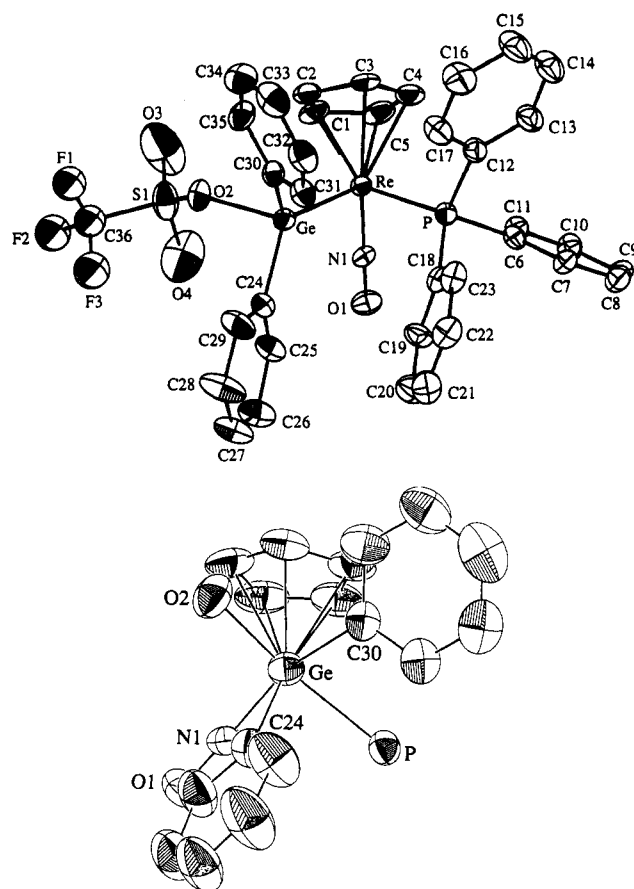


Figure 1. Crystal structure of $(\eta^5\text{-C}_5\text{H}_5)\text{Re}(\text{NO})(\text{PPh}_3)(\text{GePh}_2\text{OTf})$ (**6**): (top) numbering diagram; (bottom) Newman-type projection down the germanium-rhenium bond with the PPh_3 phenyl rings and CF_3SO_2 moiety omitted.

equiv of pyridine- d_5 at -80°C . Equilibration to $10\text{-}d_5$ was complete in less than 5 min, as assayed by ^1H NMR spectroscopy. An analogous, rapid substitution occurred with 4-methylpyridine to give **11**, but no reaction occurred with 4-pyridinecarboxaldehyde.

2. Crystal Structure of Triflate-Substituted Germyl Complex 6. In order to help interpret the dynamic NMR properties of **6** described below, a crystal structure determination was executed. X-ray data were collected under the conditions summarized in Table II. Refinement, described in the Experimental Section, yielded the structures shown in Figure 1. Atomic coordinates, bond distances, and bond angles are summarized in Tables III and IV.

In order to quantify certain geometric features in **6**, selected torsion angles were calculated (Table IV). For example, an anti relationship of the triflate and PPh_3 groups was evident (Figure 1, bottom). Accordingly, the P-Re-Ge-O2 torsion angle was found to be $173.9(3)^\circ$. Also, the P-Re-Ge plane appeared to bisect the C24-Ge-C30 linkage. As expected, the P-Re-Ge-C24 and P-Re-Ge-C30 torsion angles were nearly equal ($76.0(5)$, $69.7(4)^\circ$).

3. Dynamic NMR Properties of 6. The observation of a single set of germanium-phenyl ^{13}C NMR resonances for **6** at room temperature suggested the operation of a dynamic process that rendered the two diastereotopic phenyl groups equivalent. Thus, variable-temperature ^{13}C NMR spectra were recorded in CD_2Cl_2 (75 MHz). At 193 K, separate resonances were found for the ipso (146.40, 144.70 ppm), ortho (134.80, 133.10 ppm), para (129.99, 129.57 ppm), and meta (128.62, 128.17 ppm) carbons. The

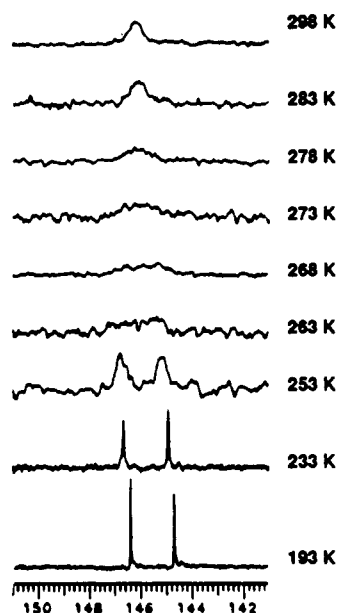
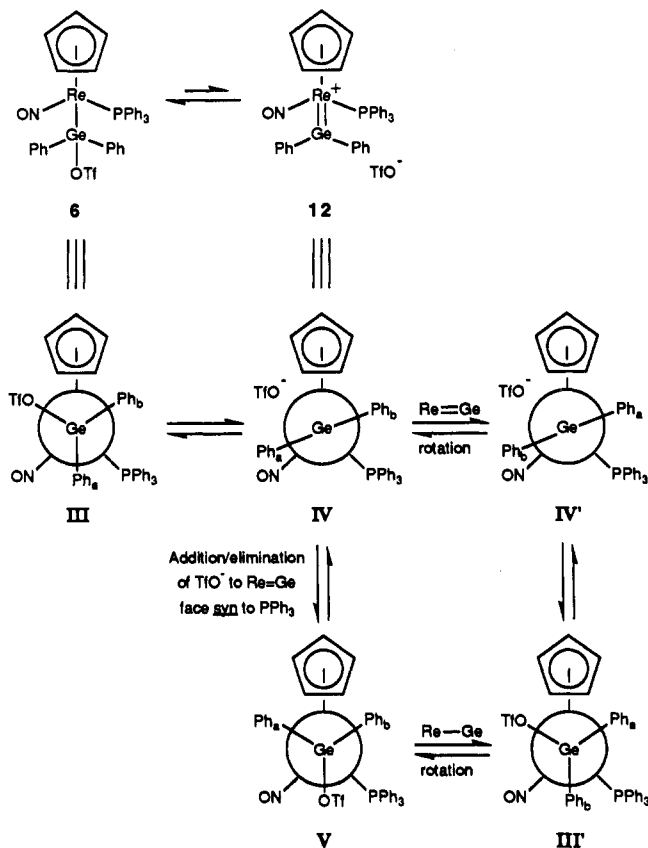


Figure 2. Variable-temperature $^{13}\text{C}\{^1\text{H}\}$ NMR spectra of $(\eta^5\text{-C}_5\text{H}_5)\text{Re}(\text{NO})(\text{PPh}_3)(\text{GePh}_2\text{OTf})$ (**6**) showing germanium-phenyl ipso carbon resonances.

Scheme II. Proposed Equilibrium of the Germyl Complex 6 and Germylene Complex 12: Possible Mechanisms for the Equivalencing of the Diastereotopic Phenyl Groups



first two decoalesced at 268 K, and the last two decoalesced near 253 K. The ipso carbon region is depicted in Figure 2.

Application of the coalescence formula¹³ to the ipso and ortho carbon resonances gave $\Delta G^\ddagger_{268\text{K}} = 12.6 \pm 0.2$ kcal

(13) Sandström, J. *Dynamic NMR Spectroscopy*; Academic Press: New York, 1982; Chapter 7.

Table I. Spectroscopic Characterization of New Rhenium Complexes

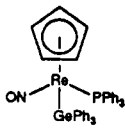
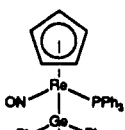
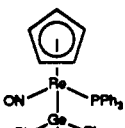
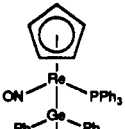
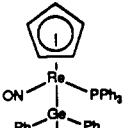
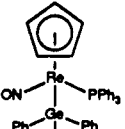
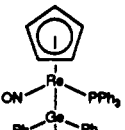
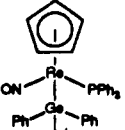
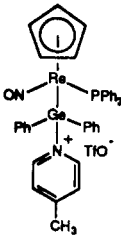
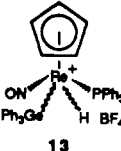
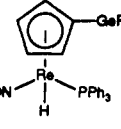
complex	IR (KBr), cm ⁻¹	¹ H NMR, ppm ^a	¹³ C{ ¹ H} NMR, ppm ^b	³¹ P{ ¹ H} NMR, ppm ^c
 3	ν_{NO} 1645 (vs)	7.29 (m, 6 H of 6 C ₆ H ₅), 7.16 (m, 18 H of 6 C ₆ H ₅), 6.90 (m, 6 H of 6 C ₆ H ₅); 4.84 (s, C ₅ H ₅)	GePh ₃ at 149.3 (s, <i>i</i>), 135.2 (s, <i>o</i>), 127.4 (s, <i>p</i>), 126.6 (s, <i>m</i>); PPh ₃ at 136.8 (d, <i>J</i> = 53.2 Hz, <i>i</i>), 133.7 (d, <i>J</i> = 10.9 Hz, <i>o</i>), 129.9 (s, <i>p</i>), 128.0 (d, <i>J</i> = 9.7 Hz, <i>m</i>); 89.0 (s, C ₅ H ₅)	20.8 (s)
 4	ν_{NO} 1664/1665 ^d (vs)	7.63–7.09 (m, 5 C ₆ H ₅), 5.05 (s, C ₅ H ₅)	GePh ₂ at 150.0 (s, <i>i</i>), 147.8 (s, <i>i</i>), 133.2 (s, <i>o</i>), 127.8 (s, <i>p</i>), 127.6 (s, <i>m</i>); PPh ₃ at 136.3 (d, <i>J</i> = 54.0 Hz, <i>i</i>), 133.5 (d, <i>J</i> = 10.9 Hz, <i>o</i>), 130.3 (s, <i>p</i>), 128.2 (d, <i>J</i> = 10.2 Hz, <i>m</i>); 89.8 (s, C ₅ H ₅)	17.1 (s)
 5	ν_{NO} 1657 (vs); ν_{GeH} 1979 (m)	7.50–7.10 (m, 5 C ₆ H ₅); 4.97 (d, <i>J</i> _{PH} = 4.6 Hz, GeH); 4.80 (s, C ₅ H ₅)	GePh ₂ at 148.1 (s, <i>i</i>), 146.9 (s, <i>i</i>), 135.7 (s, <i>o</i>), 135.2 (s, <i>o</i>), 127.9 (s, <i>p</i>), 127.7 (s, <i>p</i>), 127.2 (s, <i>m</i>), 127.8 (s, <i>m</i>); PPh ₃ at 136.9 (d, <i>J</i> = 53.7 Hz, <i>i</i>), 133.9 (d, <i>J</i> = 11.1 Hz, <i>o</i>), 130.5 (s, <i>p</i>), 128.5 (d, <i>J</i> = 10.2 Hz, <i>m</i>); 88.1 (s, C ₅ H ₅)	21.2 (s)
 6	ν_{NO} 1678/1683 ^d (vs); $\nu_{\text{CF}_3\text{SO}_3}$ 1331/1339 ^d (vs), 1234 (s), 1200 (s)	7.31 (m, 13 H of 5 C ₆ H ₅), 7.16 (m, 6 H of 5 C ₆ H ₅), 7.00 (m, 6 H of 5 C ₆ H ₅); 5.30 (s, C ₅ H ₅)	GePh ₂ at 146.3 (s, br, <i>i</i>), 134.1 (s, br, <i>o</i>), 129.6 (s, <i>p</i>), 128.3 (s, <i>m</i>); PPh ₃ at 136.1 (d, <i>J</i> = 55.4 Hz, <i>i</i>), 133.5 (d, <i>J</i> = 11.1 Hz, <i>o</i>), 131.0 (s, <i>p</i>), 128.8 (d, <i>J</i> = 10.8 Hz, <i>m</i>); 119.4 (q, <i>J</i> _{CF} = 319.4 Hz, CF ₃); 90.3 (s, C ₅ H ₅)	15.7 (s)
 7	ν_{NO} 1655 (vs)	7.52–7.09 (m, 5 C ₆ H ₅); 4.96 (s, C ₅ H ₅)	GePh ₂ at 150.9 (d, <i>J</i> _{CF} = 15.7 Hz, <i>i</i>), 148.5 (d, <i>J</i> _{CF} = 12.7 Hz, <i>i</i>), 133.0 (d, <i>J</i> _{CF} = 2.9 Hz, <i>o</i>), 132.5 (d, <i>J</i> _{CF} = 2.3 Hz, <i>o</i>), 127.8 (s, <i>m</i>), 127.7 (s, <i>p</i>); PPh ₃ at 137.1 (d, <i>J</i> = 54.3 Hz, <i>i</i>), 133.7 (d, <i>J</i> = 11.3 Hz, <i>o</i>), 130.4 (d, <i>J</i> = 2.2 Hz, <i>p</i>), 128.4 (d, <i>J</i> = 10.5 Hz, <i>m</i>); 88.5 (s, C ₅ H ₅)	19.2 (s)
 8	ν_{NO} 1665 (vs)	7.35–7.01 (m, 5 C ₆ H ₅); 5.04 (s, C ₅ H ₅)	GePh ₂ at 149.0 (s, <i>i</i>), 147.1 (s, <i>i</i>), 133.9 (s, <i>o</i>), 133.8 (s, <i>o</i>), 128.0 (s, <i>p</i>), 127.9 (s, <i>p</i>), 127.7 (s, <i>m</i>); PPh ₃ at 136.3 (d, <i>J</i> = 54.1 Hz, <i>i</i>), 133.8 (d, <i>J</i> = 11.2 Hz, <i>o</i>), 130.4 (d, <i>J</i> = 2.5 Hz, <i>p</i>), 128.4 (d, <i>J</i> = 10.8 Hz, <i>m</i>); 90.6 (s, C ₅ H ₅)	16.8 (s)
 9	ν_{NO} 1663 (vs)	7.35–6.95 (m, 5 C ₆ H ₅); 5.15 (s, C ₅ H ₅)	GePh ₂ at 147.8 (s, <i>i</i>), 145.5 (s, <i>i</i>), 134.5 (s, <i>o</i>), 134.4 (s, <i>o</i>), 128.1 (s, <i>p</i>), 128.1 (s, <i>p</i>), 127.6 (s, <i>m</i>); PPh ₃ at 136.2 (d, <i>J</i> = 54.1 Hz, <i>i</i>), 133.6 (d, <i>J</i> = 10.8 Hz, <i>o</i>), 130.5 (s, <i>p</i>), 128.5 (d, <i>J</i> = 10.4 Hz, <i>m</i>); 91.7 (s, C ₅ H ₅)	16.6 (s)
 10	ν_{NO} 1674/1682 ^d (vs); ν_{CF_3} 1271/1271 ^d (vs), 1224 (s), 1150 (s), 1045 (s); $\delta_{\text{C}_6\text{H}_5\text{N}}$ 1610 (s)	8.67 (d, <i>J</i> = 5.1 Hz, 2 H of C ₆ H ₅ N), 8.16 (t, <i>J</i> = 7.7 Hz, 1 H of C ₆ H ₅ N), 7.74 (t, <i>J</i> = 6.9 Hz, 2 H of C ₆ H ₅ N); 7.60–7.11 (m, 16 H of 5 C ₆ H ₅), 6.97 (m, 9 H of 5 C ₆ H ₅); 5.19 (s, C ₅ H ₅)	C ₆ H ₅ N at 147.2 (s, <i>o</i>), 143.0 (s, <i>p</i>), 127.4 (s, <i>m</i>); GePh ₂ at 143.9 (s, <i>i</i>), 143.2 (s, <i>i</i>), 134.4 (s, <i>o</i>), 133.9 (s, <i>o</i>), 130.1 (s, <i>p</i>), 129.6 (s, <i>p</i>), 129.4 (s, <i>m</i>), 128.8 (s, <i>m</i>); PPh ₃ at 135.1 (d, <i>J</i> = 55.9 Hz, <i>i</i>), 133.4 (d, <i>J</i> = 10.9 Hz, <i>o</i>), 131.1 (s, <i>p</i>), 128.8 (d, <i>J</i> = 10.7 Hz, <i>m</i>); 121.0 (q, <i>J</i> _{CF} = 321.0 Hz, CF ₃); 90.3 (s, C ₅ H ₅)	13.1 (s)

Table I (Continued)

complex	IR (KBr), cm ⁻¹	¹ H NMR, ppm ^a	¹³ C[¹ H] NMR, ppm ^b	³¹ P[¹ H] NMR, ppm ^c
	ν_{NO} 1675 (vs); $\nu_{\text{CF}_3\text{SO}_3}$ 1267 (vs), 1224 (s), 1151 (s), 1031 (s); $\delta_{\text{C}_6\text{H}_7\text{N}}$ 1626 (s)	8.49 (d, $J = 6.5$ Hz, 2 H of $\text{C}_5\text{H}_4\text{N}$), 7.51 (d, $J = 6.5$ Hz, 2 H of $\text{C}_5\text{H}_4\text{N}$); 7.40–7.11 (m, 16 H of 5 C_6H_5), 6.96 (m, 9 H of 5 C_6H_5); 5.18 (s, C_5H_5); 2.50 (s, CH_3)	$\text{C}_5\text{H}_4\text{N}$ at 156.4 (s, p), 146.4 (s, o), 127.3 (s, m); GePh_2 at 144.0 (s, i), 143.2 (s, i), 134.3 (s, o), 133.9 (s, o), 130.0 (s, p), 129.4 (s, p), 129.3 (s, m), 128.0 (s, m); PPh_3 at 135.1 (d, $J = 55.8$ Hz, i), 133.4 (d, $J = 11.0$ Hz, o), 131.0 (s, p), 128.7 (d, $J = 10.9$ Hz, m); 121.0 (q, $J_{\text{CF}} = 320.7$ Hz, CF_3); 90.1 (s, C_5H_5); 21.7 (s, CH_3)	13.3 (s)
	ν_{NO} 1760 (vs); ν_{ReH} 1964 (w)	7.78–7.03 (m, 6 C_6H_5); 5.78 (s, C_5H_5); -1.58 (dd, $J_{\text{HP}} = 41.8$ Hz, $J = 2.7$ Hz, ReH) ^e	GePh_3 at 141.2 (s, i), 141.1 (s, i), 140.9 (s, i), 132.5 (s, o), 132.4 (s, o), 129.7 (s, p), 129.4 (s, m), 129.2 (s, m); PPh_3 at 133.1 (d, $J = 10.6$ Hz, o), 131.2 (d, $J = 3.1$ Hz, p), 130.0 (d, $J = 11.8$ Hz, m); 97.4 (s, C_5H_5) ^f	13.9 (s) ^e
	ν_{NO} 1642 (vs); ν_{ReH} 1962 (m); ν_{GeH} 1962 (m)	7.93–6.66 (m, 6 C_6H_5); 5.81 (s, GeH); C_5H_4 (m, br) at 5.14, 4.90, 4.74, 4.62; -9.66 (d, $J_{\text{HP}} = 29.2$ Hz, ReH)	GePh_2 at 145.5 (s, i), 134.0 (s, o), 127.5 (s, p), 127.0 (s, m); PPh_3 at 137.1 (d, $J = 52.6$ Hz, i), 132.6 (d, $J = 10.7$ Hz, o), 128.9 (s, p), 127.2 (d, $J = 11.0$ Hz, m); C_5H_4 at 91.6 (s), 89.0 (s), 88.8 (s), 87.3 (s), 86.8 (s)	26.8 (s)

^a At 300 MHz and ambient probe temperature in CD_2Cl_2 and referenced to internal $\text{Si}(\text{CH}_3)_4$. ^b At 75 MHz and ambient probe temperature in CD_2Cl_2 and referenced to internal $\text{Si}(\text{CH}_3)_4$. All couplings are to phosphorus unless noted otherwise. Assignments of phenyl carbon resonances were made as described in footnote c of Table I in: Buhro, W. E.; Georgiou, S.; Fernández, J. M.; Patton, A. T.; Strouse, C. E.; Gladysz, J. A. *Organometallics* 1986, 5, 956. ^c At 121 MHz and ambient probe temperature in CD_2Cl_2 and referenced to external 85% H_3PO_4 . ^d The second value is from a spectrum taken in CH_2Cl_2 . ^e Spectrum taken at 0 °C. ^f PPh_3 ipso carbon not observed.

Table II. Summary of Crystallographic Data for $(\eta^5\text{-C}_5\text{H}_5)\text{Re}(\text{NO})(\text{PPh}_3)(\text{GePh}_2\text{OTf})(6)$

mol formula	$\text{C}_{36}\text{H}_{30}\text{F}_3\text{GeNO}_4\text{PReS}$
mol wt	919.468
cryst syst	monoclinic
space group	$P2_1/n$ (No. 14)
cell dimens (16 °C)	
a, Å	16.908 (3)
b, Å	20.160 (3)
c, Å	10.437 (2)
β , deg	93.82 (2)
V, Å ³	3549.54
Z	4
d_{calc} , g/cm ³ (16 °C)	1.72
d_{obs} , g/cm ³ (27 °C)	1.70
cryst dimens, mm	0.36 × 0.35 × 0.31
diffractometer	Syntex P1
radiation (λ , Å)	Mo K α (0.71073)
data collection method	θ - 2θ
scan speed, deg/min	variable, 3.0–8.0
no. of rflns measd	5993
range/indices (hkl)	0–19, 0–23, -11 to +11
scan range	$K\alpha_1 - 1.0$ to $K\alpha_2 + 1.0$
2θ limit, deg	3.0–48.0
total bkgd time/scan time	0.5
no. of rflns between stds	98
total no. of unique data	5785
no. of obsd data, $I > 3\sigma(I)$	3990
abs coeff, cm ⁻¹	44.433
min abs cor	72.323
max abs cor	99.942
no. of variables	397
goodness of fit	3.23
R (averaging; I_o , F_o)	0.0123, 0.0115
$R = \sum F_o - F_c / \sum F_o $	0.0482
$R_w = [\sum w(F_o - F_c)^2 / \sum w F_o ^2]^{1/2}$	0.0562
$\Delta/\sigma(\text{max})$	0.06
$\Delta\rho(\text{max})$, e/Å ³	1.05 (0.93 Å from Re)

mol⁻¹. Similar variable-temperature behavior was observed in the less polar solvent chlorobenzene (ipso resonances at 146.68 and 144.92 ppm, 233 K).¹⁴ However, the coa-

lence temperature (323 K) and $\Delta G^\ddagger_{\text{T}(\text{coal})}$ (15.3 ± 0.2 kcal mol⁻¹) increased significantly. As will be elaborated in the Discussion, these data suggest the equilibration of 6 with the germylene complex $[(\eta^5\text{-C}_5\text{H}_5)\text{Re}(\text{NO})(\text{PPh}_3)(=\text{GePh}_2)]^+\text{TfO}^-$ (12, Scheme II).

4. Other Reactions of Germyl Complexes. Compounds with germanium-phenyl bonds have previously been observed to react with acids HX to give compounds with germanium-X bonds and benzene.^{9b} Such electrophilic cleavage reactions are commonly viewed as proceeding via ipso carbon protonation. We sought to probe similar reactions of the preceding phenylgermyl complexes with HX, where X⁻ would be a poorly coordinating anion. Accordingly, dichloromethane solutions of 3 were treated with $\text{HBF}_4 \cdot \text{OEt}_2$ at -78 °C. However, workup gave the germyl hydride complex $[(\eta^5\text{-C}_5\text{H}_5)\text{Re}(\text{NO})(\text{PPh}_3)(\text{GePh}_3)(\text{H})]^+\text{BF}_4^-$ (13) in 43% yield (Scheme III).^{15,16} Small amounts of benzene were observed in ¹H NMR monitored experiments, but 13 was the only cyclopentadienyl-containing product formed in appreciable quantity.

Complex 13 exhibited an IR ν_{NO} absorption (1764 cm⁻¹) similar to those of the previously reported square-pyramidal cyclopentadienylrhenium complexes $[(\eta^5\text{-C}_5\text{H}_5)\text{Re}(\text{NO})(\text{PPh}_3)(\text{X})(\text{Y})]^{n+}$.^{10,17} A weak IR ν_{ReH} absorption was also observed (1964 cm⁻¹). Complex 13 appeared to be a single geometric isomer, but the ¹H NMR chemical shift of the hydride ligand varied somewhat with temperature (δ (CD_2Cl_2): -85 °C, -1.88 br d, $J_{\text{HP}} = 39.7$ Hz; 0 °C, -1.58

(14) Abboud, J. L. M.; Kamlet, M. J.; Taft, R. W. *Prog. Phys. Org. Chem.* 1981, 13, 485 (Tables 10 and 35).

(15) (a) Schubert, U. *Adv. Organomet. Chem.* 1990, 30, 151. (b) Lichtenberger, D. L.; Rai-Chaudhuri, A. *J. Chem. Soc., Dalton Trans.* 1990, 2161.

(16) (a) Carré, F.; Colomer, E.; Corriu, R. J. P.; Vioux, A. *Organometallics* 1984, 3, 1272. (b) Dong, D. F.; Hoyano, J. K.; Graham, W. A. *G. Can. J. Chem.* 1981, 59, 1455.

(17) Fernández, J. M.; Gladysz, J. A. *Organometallics* 1989, 8, 207.

Table III. Atomic Coordinates and Equivalent Isotropic Thermal Parameters for $(\eta^5\text{-C}_5\text{H}_5)\text{Re}(\text{NO})(\text{PPh}_3)(\text{GePh}_2\text{OTf})$ (6)^a

atom	x	y	z	B, Å ²
Re	0.08868 (3)	0.10159 (2)	0.20753 (4)	3.008 (8)
Ge	0.22306 (7)	0.12196 (6)	0.3084 (1)	3.41 (3)
S1	0.2291 (3)	-0.0082 (2)	0.4920 (5)	6.8 (1)
P	0.0966 (2)	0.1885 (2)	0.0568 (3)	3.21 (6)
F1*	0.3278 (0)	0.0138 (0)	0.6881 (0)	7
F2*	0.3238 (0)	-0.0865 (0)	0.6217 (0)	8
F3*	0.3787 (0)	-0.0141 (0)	0.5331 (0)	9
O1	0.1345 (6)	0.0000 (5)	0.0213 (9)	5.1 (2)
O2	0.2408 (6)	0.0623 (5)	0.4649 (9)	5.2 (2)
O3	0.1648 (9)	0.979 (1)	0.555 (2)	17.9 (6)
O4	0.240 (1)	0.9503 (7)	0.380 (2)	13.3 (6)
N1	0.1190 (6)	0.0424 (5)	0.0970 (9)	3.5 (2)
C1	0.0175 (8)	0.0473 (8)	0.360 (1)	5.3 (3)
C2	0.0493 (7)	0.1058 (8)	0.415 (1)	4.6 (3)
C3	0.0176 (8)	0.1621 (8)	0.346 (1)	5.1 (3)
C4	-0.0348 (8)	0.1373 (8)	0.244 (1)	5.3 (3)
C5	-0.0358 (8)	0.0665 (8)	0.252 (1)	5.5 (3)
C6	0.0390 (7)	0.1732 (6)	-0.096 (1)	3.6 (3)
C7	0.0474 (8)	0.2181 (7)	-0.197 (1)	4.5 (3)
C8	0.0017 (9)	0.2067 (8)	-0.313 (1)	5.2 (3)
C9	-0.0492 (9)	0.1527 (7)	-0.329 (1)	4.8 (3)
C10	-0.0558 (8)	0.1098 (7)	-0.226 (1)	4.7 (3)
C11	-0.0131 (8)	0.1192 (6)	-0.108 (1)	4.0 (3)
C12	0.0556 (8)	0.2664 (6)	0.111 (1)	4.0 (3)
C13	-0.0188 (9)	0.2886 (7)	0.063 (1)	5.1 (3)
C14	-0.050 (1)	0.3475 (8)	0.112 (2)	6.6 (4)
C15	-0.009 (1)	0.3830 (9)	0.207 (2)	7.6 (5)
C16	0.067 (1)	0.3605 (8)	0.257 (2)	7.0 (4)
C17	0.0990 (9)	0.3012 (7)	0.210 (2)	5.5 (3)
C18	0.1929 (8)	0.2089 (6)	-0.002 (1)	3.8 (3)
C19	0.2340 (8)	0.1559 (7)	-0.055 (1)	4.9 (3)
C20	0.3064 (9)	0.1662 (8)	-0.105 (2)	6.5 (4)
C21	0.3384 (9)	0.2303 (8)	-0.105 (2)	6.4 (4)
C22	0.2973 (9)	0.2822 (8)	-0.056 (1)	5.5 (3)
C23	0.2234 (9)	0.2729 (7)	-0.004 (1)	4.8 (3)
C24	0.3195 (7)	0.0962 (7)	0.232 (1)	4.1 (3)
C25	0.3173 (9)	0.0420 (7)	0.147 (2)	5.7 (4)
C26	0.388 (1)	0.0242 (8)	0.086 (2)	7.1 (4)
C27	0.457 (1)	0.0584 (9)	0.119 (2)	7.5 (5)
C28	0.462 (1)	0.109 (1)	0.206 (2)	9.4 (6)
C29	0.3914 (8)	0.1279 (9)	0.262 (2)	6.8 (4)
C30	0.2443 (7)	0.2019 (6)	0.410 (1)	3.7 (3)
C31	0.2778 (8)	0.2576 (7)	0.356 (1)	4.5 (3)
C32	0.2835 (9)	0.3183 (8)	0.421 (2)	6.0 (4)
C33	0.257 (1)	0.3234 (9)	0.543 (2)	7.3 (4)
C34	0.226 (1)	0.2681 (9)	0.604 (2)	6.7 (4)
C35	0.2187 (9)	0.2069 (8)	0.537 (1)	5.6 (4)
C36*	0.3194 (0)	-0.0235 (0)	0.5935 (0)	6

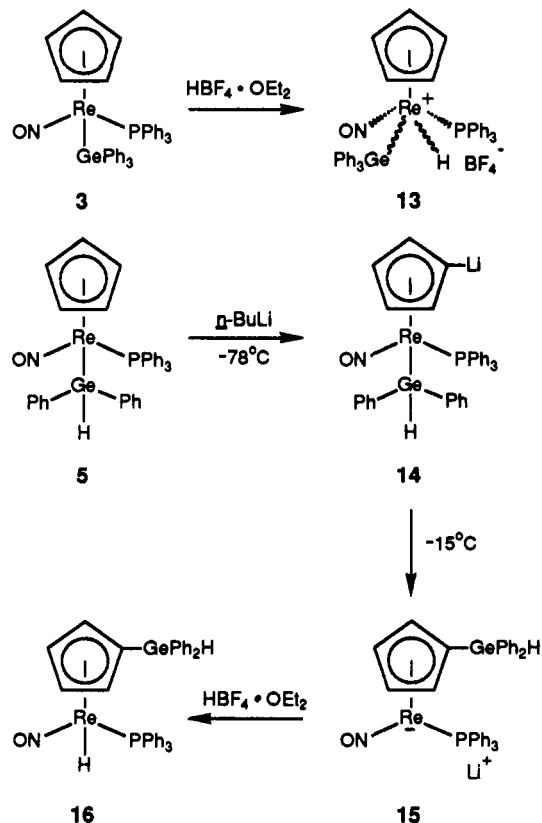
^a Anisotropically refined atoms are given in the form of the isotropic equivalent displacement parameter defined as $4/3[a^2B(1,1) + b^2B(2,2) + c^2B(3,3) + ab(\cos \gamma)B(1,2) + ac(\cos \beta)B(1,3) + bc(\cos \alpha)B(2,3)]$. Starred atoms were located but not refined.

dd, $J_{\text{HP}} = 41.8$ Hz, $J = 2.7$ Hz;¹⁸ 35 °C, -1.45 d, $J_{\text{HP}} = 42.3$ Hz). The magnitude of the J_{HP} value (40–42 Hz) suggested, by analogy to the known dihydride complex *cis*- $[(\eta^5\text{-C}_5\text{H}_5)\text{Re}(\text{NO})(\text{PPh}_3)(\text{H})_2]^+\text{BF}_4^-$ ($J_{\text{H(cis)P}} = 27\text{--}33$ Hz, $J_{\text{H(trans)P}} = 7$ Hz), that the hydride ligand was *cis* to the PPh_3 ligand.^{16,17} The bulky germyl ligand was in turn presumed to be *trans* to the PPh_3 ligand. This would place the germyl and hydride ligands *cis*—a feature often found in related germyl and silyl hydride complexes.^{15,16a}

The hydridogermyl complex $(\eta^5\text{-C}_5\text{H}_5)\text{Re}(\text{NO})(\text{PPh}_3)(\text{GePh}_2\text{H})$ (5) and *n*-BuLi (1.0 equiv, THF) were reacted in an NMR tube at -78 °C (Scheme III). Quantitative

Table IV. Selected Bond Lengths (Å), Bond Angles (deg), and Torsion Angles (deg) for $(\eta^5\text{-C}_5\text{H}_5)\text{Re}(\text{NO})(\text{PPh}_3)(\text{GePh}_2\text{OTf})$ (6)

Re-Ge	2.4738 (6)	P-C12	1.824 (5)
Re-P	2.364 (1)	P-C18	1.824 (5)
Re-N1	1.759 (4)	Re-C1	2.328 (5)
N1-O1	1.205 (5)	Re-C2	2.307 (5)
Ge-O2	2.034 (4)	Re-C3	2.291 (5)
Ge-C24	1.934 (5)	Re-C4	2.264 (5)
Ge-C30	1.952 (5)	Re-C5	2.297 (5)
S1-O2	1.465 (4)	C1-C2	1.405 (8)
S1-O3	1.334 (6)	C1-C5	1.443 (9)
S1-O4	1.458 (7)	C2-C3	1.426 (8)
S1-C36	1.826 (2)	C3-C4	1.432 (8)
P-C6	1.835 (5)	C4-C5	1.430 (9)
Ge-Re-P	93.94 (3)	O1-S1-O4	112.0 (3)
Ge-Re-N1	95.3 (1)	O2-S1-C36	99.2 (2)
P-Re-N1	92.0 (1)	O3-S1-O4	115.9 (6)
Re-N1-O1	175.3 (4)	O3-S1-C36	110.9 (4)
Re-Ge-O2	109.0 (1)	O4-S1-C36	102.8 (8)
Re-Ge-C24	123.7 (2)	Re-P-C6	113.7 (2)
Re-Ge-C30	120.0 (1)	Re-P-C12	113.0 (2)
O2-Ge-C24	95.2 (2)	Re-P-C18	118.8 (2)
O2-Ge-C30	92.2 (2)	C6-P-C12	102.9 (2)
C24-Ge-C30	108.5 (2)	C6-P-C18	100.4 (2)
Ge-C24-C25	118.7 (4)	C12-P-C18	106.1 (2)
Ge-C24-C29	122.0 (4)	C2-C1-C5	107.2 (6)
Ge-C30-C31	120.3 (4)	C1-C2-C3	109.9 (5)
Ge-C30-C35	120.6 (4)	C2-C3-C4	106.9 (6)
Ge-O2-S1	135.6 (3)	C3-C4-C5	108.2 (6)
O2-S1-O3	114.1 (5)	C1-C5-C4	107.8 (6)
P-Re-Ge-O2	173.9 (3)		
P-Re-Ge-C24	-76.0 (5)		
P-Re-Ge-C30	69.7 (4)		
N1-Re-Ge-O2	-93.8 (4)		
N1-Re-Ge-C24	16.4 (6)		
N1-Re-Ge-C30	162.1 (5)		
C30-Ge-C24-C25	-176.2 (11)		
C30-Ge-C24-C29	6.8 (14)		

Scheme III. Syntheses of Hydride Complexes from Germyl Complexes

(18) We were unable to assign the smaller apparent J_{HP} in the 0 °C spectrum. Also, the germanium-phenyl groups gave complex ¹³C NMR resonance patterns that varied with temperature. At 35 °C, the germanium-phenyl ipso carbons gave a broad resonance. However, at 0 °C the ipso carbons gave three resonances. These remained virtually unchanged at -85 °C.

conversion to the lithiocyclopentadienyl complex (η^5 -C₅H₄Li)Re(NO)(PPh₃)(GePh₂H) (14) occurred over the course of several minutes, as assayed by ³¹P NMR spectroscopy (24.1 ppm). Such 2–4 ppm downfield shifts have previously been shown to be diagnostic of cyclopentadienyl ligand lithiation in this series of compounds.^{8,19}

Complex 14 was kept for 1 h at –25 °C and then 2 h at –15 °C. Complete conversion to the rhenium-centered anion Li⁺(η^5 -C₅H₄GePh₂H)Re(NO)(PPh₃)[–] (15) occurred, as assayed by the characteristic ³¹P NMR chemical shift (45.6 ppm; cf. 2, 47.2 ppm).^{8,19} The sample was cooled to –78 °C, and HBF₄·OEt₂ was added. Workup of an analogous preparative reaction mixture gave the germylcyclopentadienyl complex (η^5 -C₅H₄GePh₂H)Re(NO)(PPh₃)(H) (16) in 46% yield. The structure of 16 followed from its ¹H and ¹³C NMR spectra (Table I), which showed resonances characteristic of a monosubstituted cyclopentadienyl ligand²⁰ and a hydride ligand.

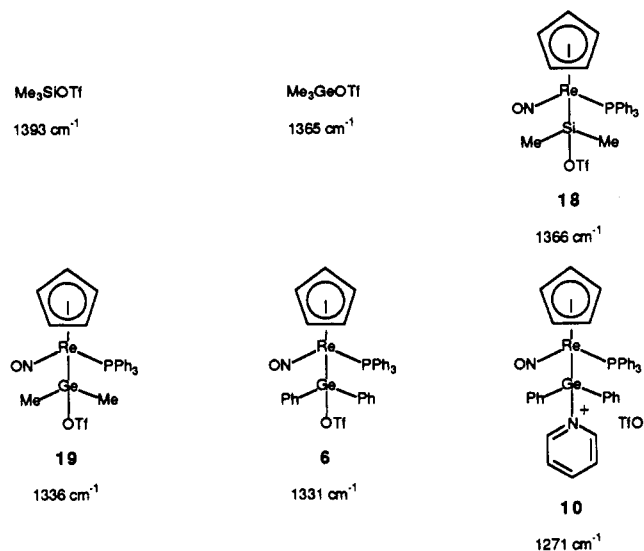
Discussion

1. Syntheses of New Germanium Compounds. The transformations outlined in Schemes I and III all have considerable literature precedent. For example, the anion 2 has previously been shown to react with silylating agents R₂SiXX' to give the silyl complexes (η^5 -C₅H₅)Re(NO)(PPh₃)(SiR₂X).^{19c} Complex 2 is also easily derivatized by other germylating agents, as reported elsewhere.^{21,22} The reduction of chlorogermyl complex 4 to hydridogermyl complex 5 has abundant analogy in organogermanium chemistry,^{9c} and related transformations have been effected with chlorosilyl and halostannyl complexes.^{2a,23} Many R₃GeH compounds react similarly to hydridogermyl complex 5 in chlorinated solvents.²⁴

The conversion of 4 to triflate 6 has precedent in the work of Tilley,^{2a} who previously showed that the reaction of Me₃SiOTf and the ruthenium chlorosilyl complex (η^5 -C₅Me₅)Ru(PMe₃)₂(SiPh₂Cl) gave Me₃SiCl and the triflate (η^5 -C₅Me₅)Ru(PMe₃)₂(SiPh₂OTf). We have observed an analogous reaction of the chlorosilyl complex (η^5 -C₅H₅)Re(NO)(PPh₃)(SiMe₂Cl).^{10b,21} The direction of these equilibria suggests that silicon–chlorine bonds in R₃SiCl compounds are considerably more covalent than silicon–chlorine and germanium–chlorine bonds in L_nM(ER₂Cl) compounds. Finally, the facile substitution of the germyl triflate group in 6 (Scheme I) parallels the reactivity of free silyl triflates.²⁵

Triphenylgermyl complex 3 reacts with HBF₄·OEt₂ (Scheme III) analogously to alkyl complexes (η^5 -C₅H₅)Re(NO)(PPh₃)(R).¹⁷ However, there are two possible limiting formulations of the product. Many *cis* germyl and stannyl hydride complexes are best represented as “ σ bond” complexes, L_nM(η^2 -H-ER₃).¹⁵ Our present data do not unequivocally distinguish between the “classical” structure [(η^5 -C₅H₅)Re(NO)(PPh₃)(GePh₃(H))]BF₄[–] (13),

Chart I. Comparison of the Highest Frequency IR $\nu_{\text{CF}_3\text{SO}_3}$ Bands in Representative Ionic and Covalent Compounds



the σ bond complex [(η^5 -C₅H₅)Re(NO)(PPh₃)(η^2 -H-GePh₃)]BF₄[–] (17), and a rapid equilibrium involving 13 and 17. However, no evidence for three-centered bonding has been found in cyclopentadienylrhenium silyl hydride complexes *cis*-(η^5 -C₅H₅)Re(CO)₂(SiR₃)(H).^{15a,16b}

Reactions involving the migration of a germyl ligand to a lithiocyclopentadienyl ligand, as for 14 → 15 in Scheme III, were first observed by Graham.²⁶ Since that time, many other examples of migrations to lithiocyclopentadienyl ligands have been found.^{8,19,27,28} In particular, this reaction occurs readily with the rhenium silyl complexes (η^5 -C₅H₄Li)Re(NO)(PPh₃)(SiR₂X).^{19c} The germyl ligand migration 14 → 15 is somewhat slower than the corresponding silyl ligand migrations.

2. Physical Properties of Triflate-Substituted Germyl Complex 6. Several properties of 6 suggest a considerable contribution to the ground state by the germylene complex resonance form [(η^5 -C₅H₅)Re(NO)(PPh₃)(=GePh₂)]⁺TfO[–] (12). First, triflate-containing compounds exhibit several IR $\nu(\text{CF}_3\text{SO}_3)$ absorptions between 1400 and 900 cm^{–1}. Previous researchers have found that the highest frequency band is typically 1395–1365 cm^{–1} in covalently bound triflates and 1280–1270 cm^{–1} in ionic triflates.²⁹ However, the corresponding absorption in 6 falls in an intermediate region (1331/1339 cm^{–1}, KBr/CH₂Cl₂), suggesting a very weakly bound triflate moiety.

Selected IR $\nu_{\text{CF}_3\text{SO}_3}$ comparisons are given in Chart I.³⁰ Syntheses of the reference silyl and germyl complexes (η^5 -C₅H₅)Re(NO)(PPh₃)(SiMe₂OTf) (18) and (η^5 -C₅H₅)Re(NO)(PPh₃)(GeMe₂OTf) (19) are described in separate studies.^{10,21,22} The data indicate that the germanium–triflate bonds in L_nM(GeR₂OTf) compounds are considerably more ionic than those in R₃GeOTf compounds. Also, germanium–triflate bonds exhibit more ionic char-

(19) (a) Heah, P. C.; Patton, A. T.; Gladysz, J. A. *J. Am. Chem. Soc.* **1986**, *108*, 1185. (b) Crocco, G. L.; Gladysz, J. A. *Chem. Ber.* **1988**, *121*, 375. (c) Crocco, G. L.; Young, C. S.; Lee, K. E.; Gladysz, J. A. *Organometallics* **1988**, *7*, 2158.

(20) (a) Johnston, P.; Loonat, M. S.; Ingham, W. L.; Carlton, L.; Coville, N. J. *Organometallics* **1987**, *6*, 2121. (b) Carlton, L.; Johnston, P.; Coville, N. J. *J. Organomet. Chem.* **1988**, *339*, 339.

(21) Lee, K. E. Ph.D. Thesis, University of Utah, 1990.

(22) Lee, K. E.; Gladysz, J. A. Manuscript in preparation.

(23) Lappert, M. F.; McGeary, M. J.; Parish, R. V. *J. Organomet. Chem.* **1989**, *373*, 107.

(24) (a) Gynane, M. J. S.; Lappert, M. F.; Riley, P. I.; Rivière, P.; Rivière-Baudet, M. *J. Organomet. Chem.* **1980**, *202*, 5. (b) Rivière, P.; Rivière-Baudet, M.; Castel, A.; Satgé, J.; Lavabre, A. *Synth. React. Inorg. Met.-Org. Chem.* **1987**, *17*, 539.

(25) Emde, H.; Domsch, D.; Feger, H.; Frick, U.; Götz, A.; Hergott, H. H.; Hofmann, K.; Kober, W.; Krägeloh, K.; Oesterle, T.; Steppan, W.; West, W.; Simchen, G. *Synthesis* **1982**, 1.

(26) Dean, W. K.; Graham, W. A. G. *Inorg. Chem.* **1977**, *16*, 1060.

(27) Other data on germyl ligand migrations: (a) Cervantes, J.; Vincenti, S. P.; Kapoor, R. N.; Pannell, K. H. *Organometallics* **1989**, *8*, 744. (b) Lobanova, I. A.; Zdanovich, V. I.; Kolobova, N. E. *Metallorg. Khim.* **1988**, *1*, 1176.

(28) Other recent references: (a) Berryhill, S. R.; Corriu, R. J. P. *J. Organomet. Chem.* **1989**, *370*, C1. (b) Nakazawa, H.; Sone, M.; Miyoshi, K. *Organometallics* **1989**, *8*, 1564.

(29) Lawrance, G. A. *Chem. Rev.* **1986**, *86*, 17.

(30) Data for Me₃SiOTf and Me₃GeOTf: (a) Roesky, H. W.; Giere, H. H. *Z. Naturforsch., B* **1970**, *25*, 773. (b) Drake, J. E.; Khasrou, L. N.; Majid, A. *J. Inorg. Nucl. Chem.* **1981**, *43*, 1473.

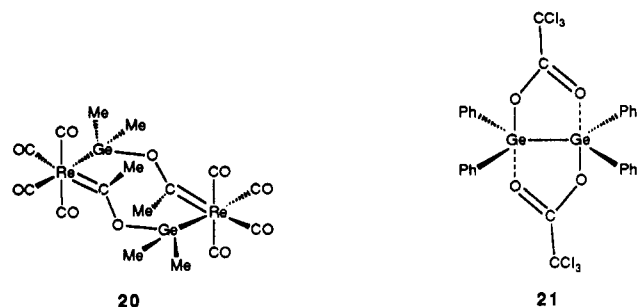


Figure 3. Relevant structurally characterized compounds.

acter than analogous silicon–triflate bonds.

The IR ν_{NO} absorption of **6** (1678/1683 cm^{-1} , KBr/ CH_2Cl_2) is at somewhat greater frequency than those of halogermyl complexes **7/4/8/9** (1655–1665 cm^{-1} , KBr). This suggests that the germyl triflate ligand is a stronger π acceptor than the halogermyl ligands. Importantly, **6** exhibits similar IR properties in KBr and CH_2Cl_2 . If a significant equilibrium amount of triflate ionization occurred in CH_2Cl_2 , a second and much higher frequency ν_{NO} absorption would be observed.

The crystal structure of **6** shows several interesting features (Figure 1). First, note that **6** exhibits the ca. 90° L–Re–L' angles (L, L' = non-cyclopentadienyl ligands) commonly observed for this formally octahedral class of compounds (Table IV).^{5a,c} Second, **6** adopts a rhenium–germanium conformation that gives an anti alignment of the Ph_3P –Re and Ge–OTf bonds. This orientation maximizes overlap of the d orbital HOMO shown in I and the Ge–OTf σ^* antibonding orbital. This type of interaction should provide considerable ionic character to the germanium–triflate bond and double-bond character to the rhenium–germanium bond.

Accordingly, the germanium atom in **6** shows a marked distortion toward a planar geometry. The sum of the Re–Ge–C24, Re–Ge–C30, and C24–Re–C30 bond angles is 352.2° —much closer to that expected for a planar trigonal atom (360°) than a tetrahedral atom (328.5°). Indeed, the disposition of the Re^+GePh_2 moiety in **6** bears a striking resemblance to that of the $\text{Re}=\text{CRR}'$ grouping in alkylidene complexes $[(\eta^5\text{-C}_5\text{H}_5)\text{Re}(\text{NO})(\text{PPh}_3)(=\text{CRR}')]\text{X}^-$ (see II).^{5a,c}

A search of the Cambridge crystallographic data base located only one other structurally characterized compound with a rhenium–germanium bond, the dimeric carbene complex **20** (Figure 3).³¹ Consistent with the preceding analysis, the rhenium–germanium bond in **6** (2.4738 (6) Å) is distinctly shorter than that in **20** (2.591 (3) Å).

No structurally characterized germanium triflates were located. However, 63 compounds with germanium–oxygen bonds were found. These gave a mean germanium–oxygen bond length of 1.814 Å—approximately 0.2 Å shorter than the germanium–triflate bond in **6** (2.034 (4) Å). With the exception of digermene **21** (Figure 3; Ge–O–C = 2.073 (2) Å, Ge–O=C = 2.314 (2) Å),³² no other compound exhibited a germanium–oxygen bond that was longer than 2.0 Å. The sum of the germanium and oxygen covalent radii (1.22–1.23 and 0.66–0.74 Å)³³ is distinctly less than 2.0 Å.

Tilley has reported the crystal structure of the triflate-substituted diphenylsilyl ruthenium complex $(\eta^5\text{-C}_5\text{Me}_5)\text{Ru}(\text{PMe}_3)_2(\text{SiPh}_2\text{OTf})$ (**22**).^{2a} He finds a similarly lengthened silicon–oxygen bond; the silicon is somewhat less distorted toward a planar geometry (sum of Ru–Si–C, Ru–Si–C', C–Si–C' bond angles 340.6°).

3. Equilibria Involving Germylene Complex 12. Although well-characterized germylene complexes are not abundant, examples of several classes have been isolated.^{1,3} The germanium is generally substituted with heteroatomic or bulky alkyl groups. Representative compounds are illustrated in Figure 4. Interestingly, isolable cationic germylene complexes are to our knowledge unknown.

The dynamic NMR properties of **6** (Figure 2) require a low-energy pathway for the exchange of the diastereotopic phenyl groups. One possibility would involve an inversion of configuration at rhenium, followed by rhenium–germanium bond rotation.³⁴ However, nearly all rhenium complexes of the type $(\eta^5\text{-C}_5\text{H}_5)\text{Re}(\text{NO})(\text{PPh}_3)(\text{X})$ exhibit excellent configurational stability at room temperature.³⁵ Also, analogous dynamic NMR behavior is not found for bromogermyl complex **8** or iodogermyl complex **9**. Thus, a phenyl-exchange pathway involving inversion of configuration at germanium is more plausible.

Scheme II shows that exchange of the phenyl groups in **6** is easily accomplished via the intermediacy of germylene complex **12**. As suggested by the crystal structure of **6**, **12** is depicted with the germylene ligand conformation shown in IV, analogous to the alkylidene ligand conformation in II. Two distinct exchange mechanisms are possible.

First, the Re=Ge double bond of **12** could rotate (IV \rightarrow IV', Scheme II). The triflate anion could then add to the germanium in IV' from a direction anti to the bulky PPh_3 ligand. This is the microscopic reverse of III \rightarrow IV and gives the product III', with exchanged phenyl groups and an inverted configuration at germanium. Alternatively, the triflate anion could add to the germanium in IV from a direction syn to the PPh_3 ligand to give V. A Re–Ge single-bond rotation would then complete the reaction coordinate for exchange. The alkylidene complexes $[(\eta^5\text{-C}_5\text{H}_5)\text{Re}(\text{NO})(\text{PPh}_3)(=\text{CRR}')]\text{X}^-$ undergo preferential nucleophilic attack from a direction anti to the PPh_3 ligand.^{5a,b,e,f} Hence, we presently favor the former mechanism.

Importantly, the ΔG^\ddagger value of 12.6 kcal mol^{-1} (CD_2Cl_2 , 268 K) for phenyl group exchange in **6** constitutes an upper limit on the free energy difference between **6** and germylene complex **12**. In actuality, ΔG is likely considerably less. Note that any of the steps connecting III and III' in Scheme II can be rate-limiting. Thus, IV might be only a few kilocalories per mole less stable than the ground state III, with the bulk of the activation energy corresponding to a rate-limiting Re=Ge bond rotation (IV \rightarrow IV').

Regardless of which step in Scheme II is rate-limiting, all transition states (except V \rightarrow III') should be more polar than triflate **6**. This rationalizes the higher ΔG^\ddagger observed in the less polar¹⁴ solvent chlorobenzene. Also, the triflate-substituted dimethylgermyl complex **19** (Chart I) exhibits similar dynamic NMR behavior.^{21,22} The ^1H NMR resonances of the diastereotopic methyl groups coalesce

(31) (a) Webb, M. J.; Bennett, M. J.; Chan, L. Y. Y.; Graham, W. A. *G. J. Am. Chem. Soc.* **1974**, *96*, 5931. (b) See also unpublished structures cited in ref 16b.

(32) Simon, D.; Häberle, K.; Dräger, M. *J. Organomet. Chem.* **1984**, *267*, 133.

(33) (a) Moeller, T. *Inorganic Chemistry*; Wiley: New York, 1982; Table 2.18. (b) *Lange's Handbook of Chemistry*, 13th ed.; Dean, J. A., Ed.; McGraw-Hill: New York, 1985; Table 3-10.

(34) A synthesis of an optically active $(\eta^5\text{-C}_5\text{H}_5)\text{Re}(\text{NO})(\text{PPh}_3)(\text{GePh}_2\text{X})$ complex would exclude facile inversion of configuration at rhenium. However, the precursor anion **2** cannot be generated in optically active form.⁸

(35) For examples, see the following papers, and references therein: (a) Dewey, M. A.; Bakke, J. M.; Gladysz, J. A. *Organometallics* **1990**, *9*, 1349. (b) Dewey, M. A.; Gladysz, J. A. *Ibid.* **1990**, *9*, 1351. (c) Merrifield, J. H.; Fernández, J. M.; Buhro, W. E.; Gladysz, J. A. *Inorg. Chem.* **1984**, *23*, 4022.

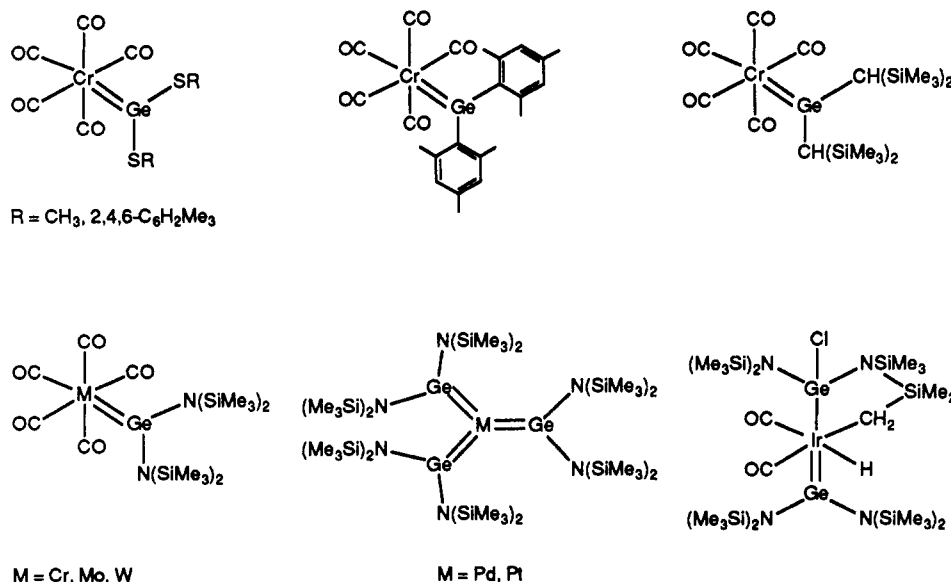


Figure 4. Some isolable germylene complexes.

at low temperatures, giving a ΔG^\ddagger value of 9.6 kcal mol⁻¹ (CD₂Cl₂, 211 K) for methyl group exchange. Finally, none of the other functionalized diphenylgermyl complexes in Scheme I exhibit dynamic NMR properties at or below room temperature. This likely reflects the superior leaving-group ability, and the poorer coordinating ability,²⁹ of the triflate anion.

We believe it likely that the substitution reactions of 6 in Scheme I, as well as the pyridine-exchange reactions of 10, also involve the intermediacy of germylene complex 12. We developed this chemistry with the hope of finding a transformation that would be slow enough at -78 °C to obtain rate data by NMR spectroscopy. Reaction orders and activation parameters can be diagnostic of dissociative substitution mechanisms. However, all reactions were essentially complete within the time of mixing.

4. Conclusion. This study has provided a high-yield entry into functionalized diphenylgermyl complexes of the formula $(\eta^5\text{-C}_5\text{H}_5)\text{Re}(\text{NO})(\text{PPh}_3)(\text{GePh}_2\text{X})$. When X is triflate (6), reactions and dynamic NMR behavior are observed that indicate a facile and only moderately endergonic equilibrium with the corresponding germylene complex $[(\eta^5\text{-C}_5\text{H}_5)\text{Re}(\text{NO})(\text{PPh}_3)(=\text{GePh}_2)]^+\text{TfO}^-$ (12). It can be anticipated that these germyl complexes will be useful precursors to a variety of unusual germanium compounds and that simple modifications of 6 may give compounds where equilibria of the type $6 \rightleftharpoons 12$ will favor germylene complexes.

Experimental Section

General Data. All reactions were carried out under a dry N₂ atmosphere. IR spectra were recorded on Perkin Elmer 1500 and Mattson Polaris (FT) spectrometers. NMR spectra were recorded on Varian spectrometers as outlined in Table I. Variable-temperature NMR experiments were conducted as previously described.³⁶ Microanalyses were performed by Galbraith Laboratories. Melting points were determined in evacuated capillaries.³⁷

Solvents were distilled (CH₂Cl₂, CHCl₃, and C₆H₅Cl from P₂O₅; benzene, ether, and THF from Na/benzophenone; hexane and heptane from sodium; pentane from LiAlH₄; cyclohexane from CaH₂) and freeze-pump-thaw degassed (3×) before use. Deu-

terated solvents were trap-to-trap distilled as follows: CD₂Cl₂, CDCl₃, and C₆D₅Cl from P₂O₅; benzene-*d*₆ from CaH₂.

Reagents were obtained as follows: *n*-BuLi (Aldrich), standardized prior to use;³⁸ Ph₃GeCl and Ph₂GeCl₂ (Alfa), HBF₄·Et₂O, LiAlH₄, (Me₂N)₃S⁺[SiMe₃F₂]⁻, and Ph₃PET⁺Br⁻ (Aldrich), [Ph₃P→N→PPh₃]⁺I⁻ (Strem) and C₆D₅N (ICN), used as purchased; Me₃SiOTf (Petrarch), distilled from CaH₂; pyridine (Baker), distilled from BaO; 4-methylpyridine (Eastman), distilled from CaH₂.

($\eta^5\text{-C}_5\text{H}_5$)Re(NO)(PPh₃)(GePh₃) (3). A Schlenk tube was charged with ($\eta^5\text{-C}_5\text{H}_5$)Re(NO)(PPh₃)(H) (1;⁸ 0.500 g, 0.919 mmol), THF (20 mL), and a stirbar. The yellow solution was cooled to -15 °C. Then *n*-BuLi (0.562 mL, 1.8 M in hexane) was added via syringe with stirring. After 0.5 h, the resulting dark red solution was cooled to -78 °C and transferred via a N₂-purged cannula to a second Schlenk tube (-78 °C) containing Ph₃GeCl (0.488 g, 1.44 mmol) and a stirbar. The solution was stirred for 0.5 h at -78 °C and turned dark orange. The tube was warmed to room temperature, and the solvent was removed in vacuo. The dark residue was extracted with benzene. The extract was filtered through a fritted funnel that had been layered with dry silica gel (2.5 cm, bottom) and Celite (0.6 cm). Solvent was removed from the filtrate by rotary evaporation, and the resulting yellow-orange residue was crystallized from CH₂Cl₂/hexane. Yellow-orange cubes formed, which were collected by filtration and dried in vacuo to give 3 (0.652 g, 0.770 mmol, 84%), mp 226.5–228 °C. Anal. Calcd for C₄₁H₃₅GeNOPRe: C, 58.09; H, 4.13. Found: C, 58.03; H, 4.21.

($\eta^5\text{-C}_5\text{H}_5$)Re(NO)(PPh₃)(GePh₂Cl) (4). Hydride complex 1 (0.600 g, 1.103 mmol), THF (20 mL), and *n*-BuLi (0.674 mL, 1.8 M in hexane) were combined as in the preparation of 3. The dark red solution was similarly transferred to a second Schlenk tube (-78 °C) containing frozen Ph₂GeCl₂ (0.493 g, 1.654 mmol) and a stirbar. The tube was shaken for 30 s (the solution turned dark yellow) and was warmed to room temperature with stirring. The solvent was removed in vacuo, and the dark residue was extracted with benzene. The extract was filtered through Celite (0.6 cm) on a fritted funnel. Solvent was removed from the filtrate by rotary evaporation, and the resulting yellow residue was extracted with cyclohexane. The extract was filtered through Celite (0.6 cm) on a fritted funnel. Solvent was removed from the filtrate by rotary evaporation. The resulting yellow residue was dissolved in a minimum amount of CH₂Cl₂, and hexane was added. The solution was concentrated by rotary evaporation. A yellow powder precipitated, which was collected by filtration and dried in vacuo to give 4 (0.728 g, 0.904 mmol, 82%), mp 210.5–212 °C. Anal. Calcd for C₃₅H₃₀ClGeNOPRe: C, 52.17; H, 3.73; Cl, 4.35. Found: C, 52.51; H, 4.07; Cl, 4.63.

(36) Dalton, D. M.; Fernández, J. M.; Emerson, K.; Larsen, R. D.; Arif, A. M.; Gladysz, J. A. *J. Am. Chem. Soc.* **1990**, *112*, 9198.

(37) Tiers, G. V. D. *J. Chem. Educ.* **1990**, *9*, 1351.

(38) Winkle, M. R.; Lansinger, J. M.; Ronald, R. C. *J. Chem. Soc., Chem. Commun.* **1980**, 87.

($\eta^5\text{-C}_5\text{H}_5$) $\text{Re}(\text{NO})(\text{PPh}_3)(\text{GePh}_2\text{H})$ (5). A Schlenk tube was charged with 4 (0.200 g, 0.248 mmol), THF (2 mL), and a stirbar. Then LiAlH_4 (0.0098 g, 0.26 mmol) was added, and the suspension was stirred for 0.5 h. The tube was transferred to a glovebox, and the suspension was filtered. Solvent was removed from the filtrate in vacuo, and the resulting yellow residue was extracted with benzene. The extract was filtered through Celite (0.6 cm) on a fritted funnel. Solvent was removed from the filtrate in vacuo, and the residue was extracted with CH_2Cl_2 . The extract was filtered, and the solvent was removed in vacuo. The residue was crystallized from CH_2Cl_2 /hexane. Yellow cubes and needles formed, which were collected by filtration and dried in vacuo to give 5 (0.168 g, 0.220 mmol, 88%), mp 217–220 °C. Anal. Calcd for $\text{C}_{35}\text{H}_{31}\text{GeNOPRe}$: C, 54.50; H, 4.02. Found: C, 54.41; H, 4.25.

($\eta^5\text{-C}_5\text{H}_5$) $\text{Re}(\text{NO})(\text{PPh}_3)(\text{GePh}_2\text{OTf})$ (6). A Schlenk tube was charged with 4 (0.642 g, 0.797 mmol), CH_2Cl_2 (6 mL), and a stirbar. Then Me_3SiOTf (0.350 mL, 0.403 g, 1.81 mmol) was added via syringe, and the solution was stirred for 0.5 h. The tube was transferred to a glovebox, and solvent was removed in vacuo. Benzene (1 mL) was added to the resulting brown residue. The residue dissolved, and then a yellow powder precipitated. The powder was collected by filtration, washed with benzene (2 mL), and crystallized from CH_2Cl_2 /hexane. Yellow needles formed, which were collected by filtration and dried in vacuo to give 6 (0.603 g, 0.656 mmol, 82%), mp 215–217 °C dec with bubbling. Anal. Calcd for $\text{C}_{35}\text{H}_{30}\text{F}_3\text{GeNO}_4\text{PReS}$: C, 47.03; H, 3.26; F, 6.20. Found: C, 46.60; H, 3.33; F, 5.85.

($\eta^5\text{-C}_5\text{H}_5$) $\text{Re}(\text{NO})(\text{PPh}_3)(\text{GePh}_2\text{F})$ (7). A 5-mm NMR tube was charged with 6 (0.020 g, 0.022 mmol) and CH_2Cl_2 (0.5 mL) and was capped with a septum. The yellow solution was cooled to –78 °C and was transferred, via a N_2 -purged cannula, to a second NMR tube (–78 °C) containing $(\text{Me}_2\text{N})_3\text{S}^+[\text{SiMe}_3\text{F}_2]^-$ (0.010 g, 0.036 mmol). The tube was warmed to room temperature and transferred to a glovebox. Solvent was removed in vacuo, and the resulting yellow residue was extracted with a minimum amount of benzene. The extract was filtered through a fritted funnel that had been layered with dry cellulose (3 cm). Solvent was removed in vacuo, and the resulting yellow residue was crystallized from CH_2Cl_2 /hexane. Yellow, irregularly shaped plates and cubes formed, which were collected by filtration and dried in vacuo to give 7 (0.016 g, 0.020 mmol, 93%), mp broad, starting at 93.0 °C dec. Anal. Calcd for $\text{C}_{35}\text{H}_{30}\text{FGeNOPRe}$: C, 53.24; H, 3.83. Found: C, 53.28; H, 3.90.

($\eta^5\text{-C}_5\text{H}_5$) $\text{Re}(\text{NO})(\text{PPh}_3)(\text{GePh}_2\text{Br})$ (8). Complex 6 (0.150 g, 0.163 mmol), CH_2Cl_2 (1.0 mL), and $\text{Ph}_3\text{PEt}^+\text{Br}^-$ (0.067 g, 0.180 mmol) were combined in a procedure analogous to that given for 7. An identical workup gave yellow, irregularly shaped plates and cubes, which were collected by filtration and dried in vacuo to give 8 (0.129 g, 0.020 mmol, 93%), mp 214–217 °C dec. Anal. Calcd for $\text{C}_{35}\text{H}_{30}\text{BrGeNOPRe}$: C, 49.43; H, 3.56. Found: C, 49.36; H, 3.50.

($\eta^5\text{-C}_5\text{H}_5$) $\text{Re}(\text{NO})(\text{PPh}_3)(\text{GePh}_2\text{I})$ (9). Complex 6 (0.088 g, 0.096 mmol), CH_2Cl_2 (1.0 mL), and $[\text{Ph}_3\text{P}^+\text{N}^-\text{PPh}_3]^+\text{I}^-$ (0.073 g, 0.105 mmol) were combined in a procedure analogous to that given for 7. An identical workup gave yellow, irregularly shaped plates and cubes, which were collected by filtration and dried in vacuo to give 9 (0.081 g, 0.090 mmol, 94%), mp 207–210 °C. Anal. Calcd for $\text{C}_{35}\text{H}_{30}\text{GeINOPRe}$: C, 46.84; H, 3.37. Found: C, 46.79; H, 3.60.

$[(\eta^5\text{-C}_5\text{H}_5)\text{Re}(\text{NO})(\text{PPh}_3)(\text{GePh}_2\text{NC}_5\text{H}_5)]^+\text{TfO}^-$ (10). A Schlenk tube was charged with 6 (0.299 g, 0.326 mmol), CH_2Cl_2 (4 mL), and a stirbar. Then pyridine (0.053 mL, 0.052 g, 0.65 mmol) was added via syringe, and the solution was stirred for 0.5 h. The tube was transferred to a glovebox, and solvent was removed in vacuo. This gave a yellow foam, which was crystallized from $\text{C}_6\text{H}_5\text{Cl}$ /pentane. Yellow needles formed, which were collected by filtration and dried in vacuo to give 10 (0.270 g, 0.270 mmol, 83%), mp 109–110 °C dec with bubbling. Anal. Calcd for $\text{C}_{41}\text{H}_{35}\text{F}_3\text{GeN}_2\text{O}_4\text{PReS}$: C, 49.31; H, 3.53; N, 2.81. Found: C, 49.31; H, 3.57; N, 2.61.

$[(\eta^5\text{-C}_5\text{H}_5)\text{Re}(\text{NO})(\text{PPh}_3)(\text{GePh}_2\text{-4-NC}_5\text{H}_4\text{Me})]^+\text{TfO}^-$ (11). Complex 6 (0.121 g, 0.132 mmol), CH_2Cl_2 (1 mL), and 4-methylpyridine (0.020 mL, 0.019 g, 0.21 mmol) were combined in a procedure analogous to that given for 10. An identical workup gave yellow needles, which were collected and dried in vacuo to give 11 (0.101 g, 0.10 mmol, 76%), mp 124–127 °C dec with bubbling. Anal. Calcd for $\text{C}_{42}\text{H}_{37}\text{F}_3\text{GeN}_2\text{O}_4\text{PReS}$: C, 49.81; H, 3.68; N, 2.77. Found: C, 50.12; H, 4.30; N, 2.61.

$[(\eta^5\text{-C}_5\text{H}_5)\text{Re}(\text{NO})(\text{PPh}_3)(\text{GePh}_2)(\text{H})]^+\text{BF}_4^-$ (13). A Schlenk tube was charged with 3 (0.100 g, 0.118 mmol), CH_2Cl_2 (2 mL), and a stirbar. The yellow solution was cooled to –78 °C, and $\text{HBF}_4\cdot\text{Et}_2\text{O}$ (0.022 mL, 0.029 g, 0.18 mmol) was added via syringe. The solution was warmed to 0 °C and stirred for 1 h. Ether was added, and a white powder precipitated. The tube was transferred to a glovebox. The powder was collected by filtration and washed with ether (3 mL). The powder turned purple within 5 min and was dried in vacuo to give 13 (0.042 g, 0.045 mmol, 43%), mp 127–129 °C dec with bubbling.

($\eta^5\text{-C}_5\text{H}_4\text{GePh}_2\text{H})\text{Re}(\text{NO})(\text{PPh}_3)(\text{H})$ (16). A Schlenk tube was charged with 5 (0.060 g, 0.078 mmol), THF (1 mL), and a stirbar. The tube was cooled to –78 °C, and $n\text{-BuLi}$ (0.052 mL, 1.65 M in hexane) was added via syringe. The yellow solution turned orange and was kept at –15 °C for 2 h. The solution became dark red and was cooled to –78 °C. Then $\text{HBF}_4\cdot\text{Et}_2\text{O}$ (0.015 mL, 0.019 g, 0.12 mmol) was added via syringe. The resulting dark yellow solution was warmed to room temperature and transferred to a glovebox. Solvent was removed in vacuo, and the dark residue was extracted with benzene. The extract was filtered. Solvent was removed in vacuo, and the resulting dark yellow residue was crystallized from CH_2Cl_2 /hexane. A yellow powder formed, which was collected by filtration and dried in vacuo to give 16 (0.207 g, 0.036 mmol, 46%), mp 139–142 °C.

Crystal Structure of 6. A yellow cube was grown by vapor diffusion of pentane into a chlorobenzene solution of 6. The crystal was sealed in a glass capillary and mounted for data collection on a Syntex P1 diffractometer. Cell constants (Table II) were obtained from 15 reflections with $25^\circ < 2\theta < 30^\circ$. The space group was determined from systematic absences ($h0l$, $l = 2n$; $0k0$, $k = 2n$) and subsequent least-squares refinement. Standard reflections showed no decay during data collection.

Lorentz and polarization corrections, and an empirical absorption correction based upon a series of ψ scans, were applied to the data. Intensities of equivalent reflections were averaged, and two reflections were rejected because their intensities differed significantly from the average. The structure was solved by the standard heavy-atom techniques with the SDP/VAX package.³⁹ Non-hydrogen atoms were refined with anisotropic thermal parameters, except for the trifluoromethyl group, which was located but not refined due to high thermal motion and disorder. Hydrogen atoms were located and added to the structure factor calculations but were not refined. Scattering factors, and $\Delta f'$ and $\Delta f''$ values, were taken from the literature.⁴⁰

Acknowledgment. We thank the NSF for support of this research.

Supplementary Material Available: A table of anisotropic thermal parameters for 6 (2 pages); a table of calculated and observed structure factors for 6 (14 pages). Ordering information is given on any current masthead page.

(39) Frenz, B. A. *The Enraf-Nonius CAD 4 SDP—A Real-time System for Concurrent X-ray Data Collection and Crystal Structure Determination*. In *Computing and Crystallography*; Schenk, H., Olthoff-Hazelkamp, R., van Koningsveld, H., Bassi, G. C., Eds.; Delft University Press: Delft, Holland, 1978; pp 64–71.

(40) Cromer, D. T.; Waber, J. T. In *International Tables for X-ray Crystallography*; Ibers, J. A., Hamilton, W. C., Eds.; Kynoch: Birmingham, England, 1974; Vol. IV, pp 72–98 and 149–150, Tables 2.2B and 2.3.1.